Polarization measurements of the Al XII resonance line emitted from micropinch plasmas of a vacuum spark discharge

F. Walden and H.-J. Kunze
Institut für Experimentalphysik V, Ruhr-Universität Bochum, 44780 Bochum, Germany

A. Petoyan and A. Urnov
P.N. Lebedev Physical Institute, Russian Academy of Sciences, 53 Leninski Prospect, Moscow, Russia

J. Dubau
Observatoire de Paris, F 92915 Meudon Principal Cedex, France
(Received 12 June 1998; revised manuscript received 11 November 1998)

Measurements of the polarization of the resonance line of Al XII ions emitted from micropinch plasmas of a low-inductance vacuum spark discharge are reported. A value of 0.12 for the polarization degree is obtained. For the interpretation of the spectra a model employing nonthermal electrons is used, which, consistent with the spectral data, provides parameters of the energy spectrum and of the anisotropy. The results show that x-ray polarization spectroscopy is a powerful tool for studying non-Maxwellian phenomena in hot dense plasmas. [S1063-651X(99)09303-4]

PACS number(s): 52.70.La, 52.25.Nr, 52.80.Vp, 34.80.Lx

I. INTRODUCTION

Polarization of continuum radiation (bremsstrahlung) in the hard x-ray spectral region was the subject of many investigations in the laboratory (see, for example, Refs. [1–4]) but also a topic of astrophysical (solar flares) observations [5,6]. Polarization is generated by anisotropic non-Maxwellian electrons, and hence of respective diagnostic potential. The importance of polarization measurements of x-ray lines for the diagnostics of deviations of the electron distribution from isotropy in a plasma was first pointed out by Haug [7,8] in the context of solar flares studies, and the first experimental observations of x-ray line polarization were indeed made on board the ''Intercosmos-IV'' satellite (1972) (see Ref. [9]). In this experiment, high-resolution spectra of iron ions were obtained simultaneously by means of two different Bragg crystals: they revealed a considerable difference of the relative intensities of lines in the vicinity of the resonance line (w) of the heliumlike ion.

The quantitative analysis, however, took almost ten years [10–13] before the results of calculations for the polarization degree P of the investigated lines excited by unidirectional electron beams became available [14,15]. Coulomb-Born exchange calculations with relativistic corrections made for the main lines of the heliumlike and lithiumlike ions observed in the spectra showed a relatively high value of the polarization P at the threshold energies E_{ex} of line excitation as compared to that for the L_α line of the hydrogenlike ion estimated by Haug [8]. This fact, along with the discovered dependence of the sign of linear polarization (directivity of the electric vector in line emission) on the type of the transition and the energy of nonthermal electrons, was used in Refs. [11,13] to develop a method for the diagnostics of anisotropic nonthermal electrons in plasmas, which is based on the measurement of double line intensity ratios (see also Ref. [16]). The theory of polarized line emission in hot plasmas excited by directive electrons was developed in Ref. [17], and results of calculations for Fe XXIV–XXV lines in the distorted wave (DW) approximation, also accounting for relativistic corrections, were presented.

A theoretical scheme for the electron impact polarization of atomic spectral lines in astrophysical plasmas, also accounting for Zeeman splitting by a magnetic field, was developed in Ref. [18] in the framework of the density matrix formalism. A general density matrix description for the investigation of the angular distribution and the polarization of atomic emission in crossed electric and magnetic fields was proposed in Ref. [19] for application to the spectroscopy of tokamak plasmas. The density matrix approach was also used in Ref. [20] for a description of an atomic ensemble in terms of two quantities, population and alignment, assigned to each atomic level for an axially symmetric plasma environment. Calculations of cross sections for the excitation of magnetic sublevels needed for the interpretation of experimental results were reported in Refs. [21–23] employing various codes, and a compilation of atomic data relevant to polarization plasma spectroscopy was given in Ref. [24].

The first direct measurements of polarization lines of the He- and Li-like ions of Sc and Fe were carried out on the EBIT source in Livermore, and the results, including their interpretation, were presented in Refs. [25] and [26]. The importance of such studies as a probe of the hyperfine interactions was also shown in Ref. [25], and the depolarization role of hf effects was estimated in Ref. [27]. The agreement of collisional characteristics obtained in the aforementioned calculations, as well as of the data measured and calculated in Refs. [25,26], indicates the reliability of the present atomic properties provided by these calculations. We have to note here that a previous disagreement with Coulomb-Born calculations remarked upon in Ref. [26] is traced to omitting the Coulomb phase in the early calculations [14]. As mentioned in Ref. [15], accounting for this effect reduces the

threshold value of the polarization degree for lines of the heliumlike ions, providing agreement with the calculations of Ref. [17] to within 5%.

During the last decade a series of line polarization experiments were performed on various hot plasma sources: solar flares [28], *Z* pinches [29], laser-produced plasmas [30,31], and tokamak plasmas [32,33]. The constant growth of interest in the polarization of line emission indicates in particular an appreciation of the importance of the information which can be derived from the x-ray spectra on nonthermal electrons in hot plasmas (see Ref. [34]). Quite a number of experiments provide evidence of distortions of the Maxwellian distribution function at high energies, or of the presence of electron beams in the plasma (see, for example, Ref. [4]). In spite of their relatively low density such energetic electrons play a substantial role for the energy balance, in the thermal conductivity and other transport coefficients, as well as in the formation of emission spectra. Taking into account nonthermal electrons in the modeling of spectra, plasma parameters deduced from a spectrum like electron temperature and density, as well as the ionization equilibrium, may be considerably changed (e.g., Refs. [13,35]). Thus for the spectroscopic diagnostics of plasmas any direct information on high energy electrons is badly needed to provide a self-consistent model of the emitting plasma for an interpretation of the experimental observations.

Many physical effects or processes result in nonthermal electrons in a plasma; examples are the presence of electric fields [36], temperature gradients [37,38], parametric instabilities [39], etc., which lead to the formation of an anisotropic distribution function characterized by a preferential direction of energetic electrons. In the case when electron-ion collisions are the dominant mechanism for the excitation of lines, this anisotropy will result in an alignment of ions along the respective direction due to unequal populations of the magnetic sublevels within an excited atomic level. Radiation from this level will then be partially polarized with a degree of polarization *P* depending on the degree of anisotropy of the non-Maxwellian electrons. Measurements of *P* thus make it possible to derive characteristics of the distribution function for nonthermal electrons in the framework of the adopted model.

Partial polarization of x-ray lines occurs when the density of nonthermal electrons at energies near the threshold energy *E* for line excitation is comparable to or larger than the density of the thermal electrons. These energies are typically of the order $(3-6)kT$. Thus the method of x-ray line polarization spectroscopy is adequate for the diagnostics of nonthermal electrons of relatively low energies of about $1-15$ keV, while the spectroscopy of high-energy photons with $E \geqslant 50$ keV emitted due to bremsstrahlung provides the best tool for studying high-energy runaway electrons.

In this paper we report the application of line polarization spectroscopy in the x-ray region to micropinch plasmas of a low-inductance vacuum spark discharge. These fast discharges through plasmas of eroded anode material are characterized by the occurrence of one or several pointlike microplasmas of extremely short lifetime emitting intensely in the x-ray region. Several mechanisms have been advanced to explain the formation of these tiny plasmas, and in their review Koshelev and Pereira [40] analyzed and discussed our respective knowledge. At present, a radiative collapse model by Vikhrev, Ivanov, and Koshelev [41] is favored, since its predictions agree quite well with experimental observations [40,42]. Other models invoked creation and heating by fast electron beams, although several observations contradict such a scheme of microplasma formation. The existence of fast electrons is certainly accepted [43], and in Ref. [44] such a beam was inferred from the polarization of emitted continuum radiation in the x-ray region during the short lifetime of the microplasma. It is generally accepted that electron beams are not responsible for the microplasmas, but are created during their formation or existence. The present study will shed further light on this problem.

In Sec. II the experiment is described, and results of measurements of the degree of polarization for the resonance and the intercombination line of Al XII are given. Section III presents a theoretical approach to the problem, and a formulation of the model used in estimating characteristics of the nonthermal electrons.

II. EXPERIMENT

A. Method of investigation

Polarization of x-ray lines emitted from a plasma is due to alignment of the emitting ions caused by the anisotropy of their excitation. Since the dominant excitation mechanism in hot plasmas is by electron-ion collisions, polarization of the lines occurs when the velocity distribution of the electrons is anisotropic. In the case of an axial symmetry of the electron velocity distribution function, the ensemble of excited ions represents an axially symmetric aligned system characterized by the unit vector $\vec{n}$ along the axis of symmetry because of the axial symmetry of the elementary collisional excitation. Such a state of an atomic system, being an incoherent superposition of magnetic sublevels (*M* components) within an excited atomic level, is mixed; and it is described by a diagonal density matrix with matrix elements representing the population of the *M* states [45,46]. The line radiation emitted from unequally populated sublevels is partially polarized with a degree of polarization depending on the degree of anisotropy of the distribution function.

The degree of polarization *P* defined as the ratio of the intensity of the polarized photons I_p to the total intensity *I* is usually expressed through the Stokes parameters η_i as follows:

$$P = \frac{I_p}{I} = \sqrt{\sum_{i=1}^{3} \eta_i^2}. \tag{1}$$

Lines emitted from an axially symmetric aligned system are linearly polarized with $\eta_1 = \eta_2 = 0$ and η_3 being defined with respect to the axis chosen in the $(\vec{k},\vec{n})$ plane perpendicular to the photon wave vector $\vec{k}$ as

$$\eta_3 = \frac{I(0°) - I(90°)}{I}, \tag{2}$$

where $I(\beta)$ denotes the intensity of the line with the electric field vector $\vec{E}$ of the polarized component oriented at the angle β to the axis. The degree of polarization is thus equal to

$$P=|\eta_3|. \tag{3}$$

The parameter $\eta_3(\theta)$ is a function of the angle $\theta=(\vec{k},\vec{n})$ characterizing the direction of line emission with respect to the axis $\vec{n}$. For $\theta=90°$ the sign of η_3 indicates the orientation of the electric vector $\vec{E}$, i.e., parallel $(+)$ or perpendicular $(-)$ to $\vec{n}$.

The Stokes parameter η_3 — its sign and absolute value $P_0=|\eta_3(90°)|$ — depend on the type of the transition and the polarization momenta of the M states determined by the electron distribution function and the characteristics of the elementary processes in the plasma. A measurement of this parameter for spectral lines provides a diagnostic tool for a quantitative analysis of the departure of the electron distribution function from an isotropic distribution.

The principle of linear polarization measurements employing Bragg spectrometry is based on the dependence of the crystal reflection coefficient $R(a)$ on the degree of polarization $P(a)$ of the incident line and the orientation of the electric vector $\vec{E}$ with respect to the incidence plane on the crystal, i.e., the azimuthal angle ϕ. For Bragg angles θ_B near 45°, this coefficient is given by [47]

$$R(a,\varphi)=\tilde{I}(a)/I(a) = C(\lambda)\left\{1-\frac{\sin^2 2\theta_B}{2}[1-P_0(a)\cos 2(\varphi-\varphi_0)]\right\}, \tag{4}$$

where $I(a)$ is the intensity of the incident line (a) and $\tilde{I}(a)$ is the intensity after reflection. The angle φ_0 is equal to either 0° or 90° for positive or negative sign of polarization (sign of η_3), respectively, and $C(\lambda)$ contains the wavelength-dependent properties of the crystal. If $R(a)$ or $I(a)$ are measured as a function of φ, the polarization $P(a)$ is readily deduced from the corresponding modulation. Various methods can be used, involving, for example, the measurement of absolute or relative line intensities. However, most sensitive and convenient from a technical point of view is a method which uses the double intensity ratio K of two lines (a) and (b) defined as

$$K(a/b,\varphi)=\frac{\tilde{i}(a/b,\varphi)}{\tilde{i}(a/b,0)}=\frac{R(a,\varphi)}{R(b,\varphi)}\frac{R(b,0)}{R(a,0)} \quad \text{with} \quad \tilde{i}(a/b,\varphi)=\tilde{I}(a)/\tilde{I}(b), \tag{5}$$

where $\tilde{i}(a/b,\varphi),\tilde{i}(a/b,0)$ are the intensity ratios of the lines (a) and (b) recorded by two Bragg crystals, their planes of incidence being rotated against each other by the angle φ. Changing φ by rotating one crystal around the line of sight yields the dependence of K on φ, and the ratio of the polarization degrees $P(a)/P(b)$ can be obtained from a proper fitting procedure. The value thus obtained depends on the parameters of nonisotropic electrons within the model proposed for the emitting plasma.

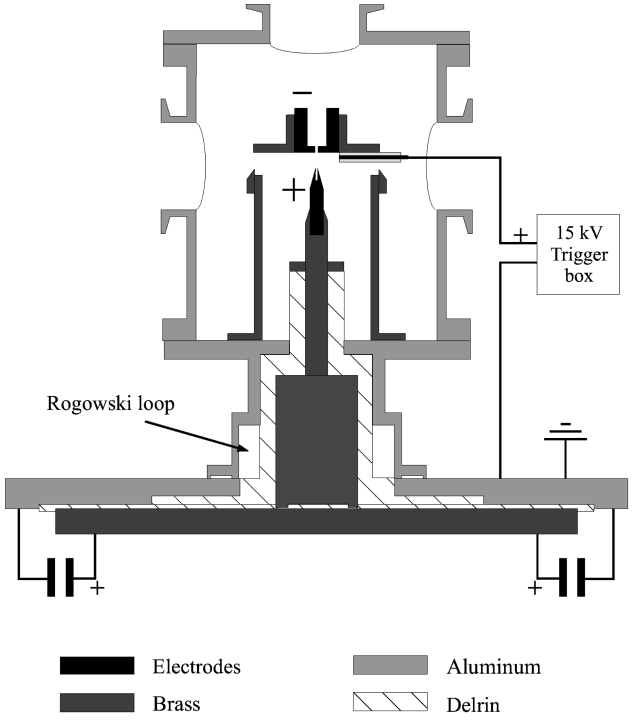

FIG. 1. Schematic of the experimental setup.

B. Experimental setup

The low-inductance vacuum spark was described in Ref. [42]. Figure 1 shows a cross-sectional view of the discharge chamber. The current is driven by discharging a capacitor bank of 11 2.4 μF capacitors (Maxwell type 31152). A charging voltage of 7.5 kV was selected, being optimum for micropinches with aluminum plasmas. However, the trigger mode and the anode shape were changed: by moving the trigger pin previously located in the center of the large-diameter cathode to a side-on configuration close to the cathode, the lifetime of the trigger pin was increased from 50 to 1000 discharges, the use of the cathode was extended from 40 to 100 discharges, and the jitter of the occurrence of a micropinch was reduced from 400 to 200 ns (see also Ref. [48]). Changing the tipped anode to one with a 1-mm hole on the axis increased the lifetime of the anode from 50 to 100 discharges, and improved the scatter of the position of the micropinches as evidenced from pinhole pictures.

Figure 2 illustrates the diagnostic setup. The derivative of the discharge current was monitored with a Rogowski loop, the occurrence of a micropinch showing up as a sudden strong dip in the signal. Simultaneously the burst of x rays is emitted, and its magnitude was used as monitor. A photomultiplier with a NE 111A scintillator was used as detector, an aluminum foil in front absorbing the soft x-ray and longer wavelength radiation. A pinhole camera with a beryllium foil recorded the position of the hot micropinches.

The resonance line of the heliumlike Al ion is at 7.7571 Å, and the requirement of a Bragg angle of $\theta_B\approx 45°$ for the optimum ratio of the crystal reflectivities of x rays polarized perpendicular and parallel to the plane of dispersion leads to crystals of a lattice spacing $2d\approx 11$ Å. We chose, therefore, ADP crystals with $2d=10.648$ Å. Two identical Bragg crystal spectrometers were built in Johann configuration, and

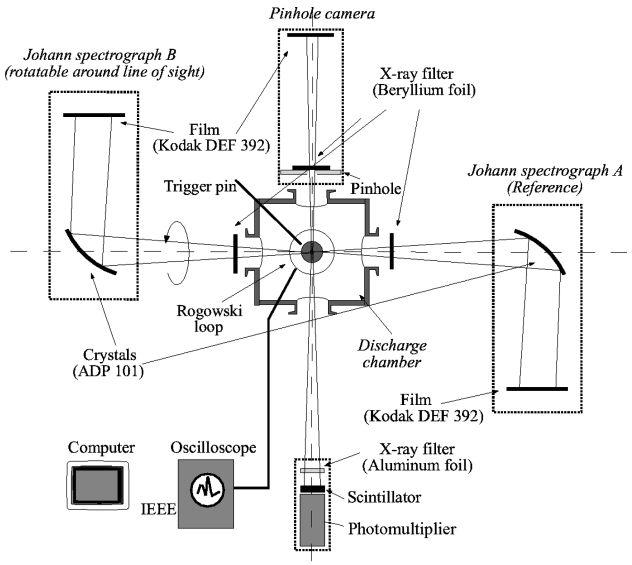

FIG. 2. Diagnostic setup.

placed opposite each other and perpendicular to the discharge axis, viewing the same plasma volume. The crystals were bent to a radius of 40 cm. One Bragg spectrometer (A) was kept in a fixed position with the plane of dispersion normal to the discharge axis, and the second spectrometer (B) was rotated in steps of 10° around the axis of the incident radiation. Recording of the spectra in the focal planes

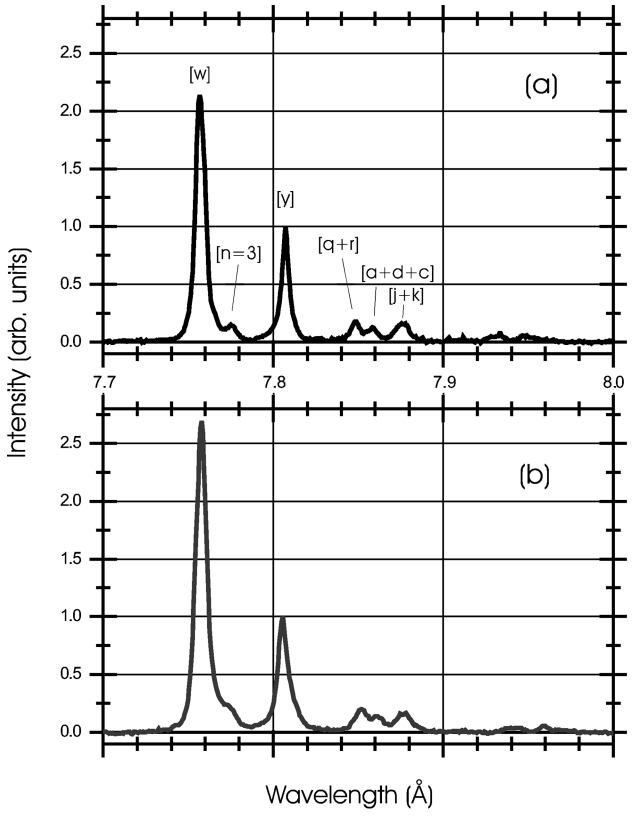

FIG. 3. Typical spectra: (a) reference spectrum recorded with fixed spectrograph and (b) spectrum recorded with a second spectrograph, which is rotated by 40°.

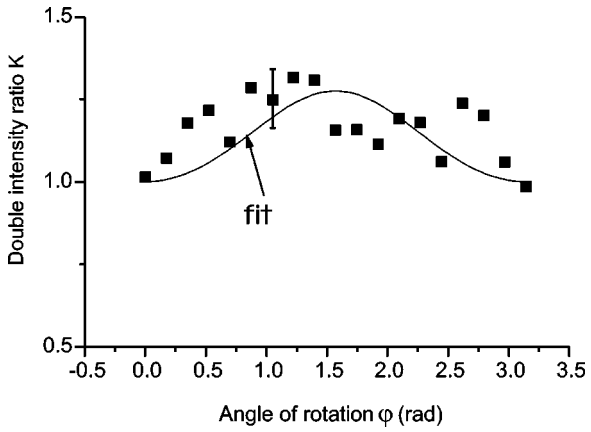

FIG. 4. Double intensity ratio K according to Eq. (5) for the resonance (w) and the intercombination (y) line of Al XII as function of angle ϕ.

was on film type Kodak DEF 392. In the x-ray region the optical density of the photographic film is practically linear in the incident flux, and hence intensity ratios of close-by lines are readily obtained from the corresponding ratios of the optical density on the film.

C. Measurements

Initially, a spectrum was recorded simultaneously with both spectrographs for each discharge, the spectrograph (B) being set at the angle $\phi=0$. The obtained spectra reflect the spectral emission integrated over the time the lines are emitted; this time corresponds to the lifetime of the hot micropinch, which is approximately 200 ps [42]. For each discharge the double intensity ratio $K(w/y,\phi)$ of resonance (w) and intercombination (y) line was readily formed and was set to $K=1$, which thus yielded the relative sensitivity calibration of both instruments. Poor discharges were readily identified by a poor dI/dt signal, by poor x-ray emission recorded with the monitor, and/or by a missing or large-sized micropinch recorded each time with the pinhole camera; they were discarded. The K values of five discharges were averaged, spectrograph (B) was then rotated by 10°, and the procedure was repeated. About 30 discharges were done with a new anode, whereby the first five discharges served for conditioning a new anode and were also discarded.

The spectra certainly varied from discharge to discharge, the mean relative uncertainty for each final K value being $\Delta K/K \leqslant 8\%$. This was acceptable but for the analysis and interpretation also the intensities of the weak dielectronic and inner-shell-excited satellites are needed, and they were indeed rather noisy. For this reason the final measurements were done by directly superposing the spectra of five discharges on film, and discarding the resulting spectrum if a poor discharge was identified in between by one of the monitors.

Figure 3 shows two such spectra as example. The plane of dispersion of the second spectrometer is rotated by 40° with respect to the top spectrum. The resonance (w) and the intercombination (y) line of heliumlike Al XII are clearly identified, as are the series of satellite lines. Figure 4 finally shows the double intensity ratio K for rotation of the spectrograph

(B) between 0° and 180°. The value of K for $\phi=180°$ is again 1, indicating the quality of the alignment and the reliability of the diagnostic procedure. The average uncertainty obtained from the original individual measurements of K is indicated by the error bar.

III. THEORETICAL APPROACH

A. Formulation of the model

We consider a plasma with an electron distribution function which is axially symmetric with respect to a unit vector $\vec{n}$ chosen along the axis of quantization (z axis). The emitting ions shall be in a quasisteady state, and are excited by collisions with unpolarized electrons having a distribution function $f(\vec{v},T)$ of the form

$$f(\varepsilon,\alpha;T)=(1-n_{\rm nt})f_{\rm th}(\varepsilon;T)f_0+n_{\rm nt}f_{\rm nt}(\varepsilon,\alpha)$$
$$\text{with}\quad f_0=\frac{1}{4\pi}\quad\text{and}\quad\cos\alpha=\frac{\vec{v}\cdot\vec{n}}{v}. \tag{6}$$

The energy ε is in threshold units $E_{\rm ex}$, i.e., $\varepsilon=E/E_{\rm ex}$, and the first term $f(\varepsilon,T)$ refers to the thermal (Maxwellian) part, whereas the second term $f_{\rm nt}(\varepsilon,\alpha)$ describes the nonthermal anisotropic distribution characterized by a pitch angle α; it is normalized as follows:

$$f_{\rm nt}(\varepsilon,\alpha)=f_{\rm nt}(\varepsilon)f(\varepsilon,\alpha), \tag{7}$$
$$\int_0^\infty f_{\rm nt}(\varepsilon)d\varepsilon=1,\quad 2\pi\int_{-1}^{1}f(\varepsilon,\alpha)d\mu=1,\quad \mu=\cos\alpha.$$

The factor $n_{\rm nt}$ is

$$n_{\rm nt}=N_{nt}/N_e\quad\text{with}\quad N_{\rm nt}+N_{th}=N_e. \tag{8}$$

$n_{\rm nt}$ is the relative density of the nonthermal electrons ($n_{\rm nt}\ll 1$), and N_e denotes the total electron density.

Expanding the pitch angle distribution function in Legendre polynomials $P_l(\mu)$, we rewrite Eq. (6) as

$$f(\varepsilon,\alpha;T)=\tilde{f}(\varepsilon)f_0+\overline{f}(\varepsilon,\alpha f_2\quad\text{with}\quad f_2=5f_0, \tag{9}$$

$$\tilde{f}(\varepsilon)=(1-n_{\rm nt})f_{\rm th}(\varepsilon)+n_{\rm nt}f_{\rm nt}(\varepsilon), \tag{10}$$
$$\overline{f}(\varepsilon,\alpha)=n_{\rm nt}f_{\rm nt}(\varepsilon)\sum_{l=2}^{\infty}\overline{f_l}(\varepsilon)P_l(\mu),$$

$$\overline{f_l}(\varepsilon)=\frac{2l+1}{2f_2}\int_{-1}^{1}f(\varepsilon,\alpha)P_l(\mu)d\mu. \tag{11}$$

TABLE I. Anisotropy parameter a as function of average pitch angle α_0.

a	1	2	3	4	7	20	40
α_0	45	38.2	30.6	24.8	19.5	15.5	11.1

For a unidirectional electron beam with $f(\varepsilon,\alpha)=(1/2\pi)\delta(1-\mu)$, we obtain $\overline{f_2}(\varepsilon)=1$, while in the general case it depends on the energy of the incident electrons. We now employ the distribution function for the nonthermal electrons as proposed by Haug [7]:

$$f(\varepsilon,\alpha)=\frac{a+1}{2\pi}(\mu)^a\theta(\pi/2-\alpha)\quad\text{with}\quad a=\varepsilon/\varepsilon_0, \tag{12}$$

where a is the parameter characterizing the degree of anisotropy at different energies, and $\theta(x)$ is the Heaviside step function. The degree of anisotropy can also be characterized by an average pitch angle α_0 which is obtained by averaging α with $f(\varepsilon,\alpha)$ of Eq. (12). The dependence of the parameter a on α_0 is given in Table I.

The energy dependence of the factor $\overline{f_2}(\varepsilon)$ is given by

$$\overline{f_2}(\varepsilon)=\frac{a}{a+3}. \tag{13}$$

For lines excited by anisotropic electron beams, the degree of polarization P_0 at the angle $\theta=90°$ (we shall also use P_0 for η_3, for simplicity) is expressed through cross sections for excitation of the M states averaged over the electron distribution function Eq. (9) with $n_{\rm nt}=1$ [14]. For the resonance (w) and the intercombination (y) line of heliumlike ions, it is given by

$$\overline{P}_0=\frac{\langle v\sigma_0(\varepsilon,\alpha)\rangle-\langle v\sigma_1(\varepsilon,\alpha)\rangle}{\langle v\sigma_0(\varepsilon,\alpha)\rangle+\langle v\sigma_1(\varepsilon,\alpha)\rangle}, \tag{14}$$

where $\sigma_i(\varepsilon,\alpha)$ are the excitation cross sections for the M states relative to the quantization axis rotated by the angle α against the vector $\vec{n}$. Using the general transformation properties of cross sections for rotation with respect to the quantization axis, $\overline{P}_0$ can be expressed through the degree of polarization of a unidirectional beam $\tilde{P}_0$ as follows:

$$\overline{P}_0=\frac{3\tilde{P}_0\beta}{3-\tilde{P}_0(1-\beta)}, \tag{15}$$

where the parameter β is defined as

$$\beta=\int v[\sigma_0(\varepsilon)-\sigma_1(\varepsilon)]f_{\rm nt}(\varepsilon)\overline{f_2}(\varepsilon)d\varepsilon\Big/\int v[\sigma_0(\varepsilon)-\sigma_1(\varepsilon)]f_{\rm nt}(\varepsilon)d\varepsilon. \tag{16}$$

In the plasma the cross sections have to be averaged over the distribution function including the Maxwellian part, and population of the M states caused by other processes should be taken into account. Assuming that this population has an isotropic character, the polarization of lines under study is related to the value from Eq. (15) by

$$P_0=\frac{3\overline{P}_0 g}{3-(1-g)\overline{P}_0} \quad \text{with} \quad g=\frac{\langle v\sigma\rangle_{\rm nt}}{X}. \tag{17}$$

Here σ is the cross section summed over all M states, and X is the total rate of excitation of the J level.

As seen from Eqs. (15)–(17), there are two factors β and g which lead to a decrease of the polarization degree P_0. The first is connected with the width of the anisotropic distribution function characterized by the averaged pitch angle α_0, and the second depends on the relative contribution of the nonthermal electrons to the total population of a J level. In order to reveal the role of these factors, we have considered two types of trial functions $f_{\rm nt}(\varepsilon)$ for the energy spectrum of these electrons: an exponential function with a sharp low-energy cutoff at an energy $\varepsilon_1=E_1/E_{\rm ex}$ and $\gamma>1$ (model A)

$$f_{\rm nt}(\varepsilon)=\frac{\gamma-1}{\varepsilon_1}\left(\frac{\varepsilon}{\varepsilon_1}\right)^{-\gamma} \quad \text{for} \quad \varepsilon\geqslant\varepsilon_1$$

and

$$f_{nt}(\varepsilon)=0 \quad \text{for} \quad \varepsilon<\varepsilon_1, \tag{18}$$

and a Maxwellian with a temperature $T_1\gg T_e$, which is widely employed for simulations of a nonthermal component of the distribution function (model B). In fact, such a high-energy Maxwellian had been identified in a vacuum spark discharge with Mo electrodes, where it was deduced from the shape of the bremsstrahlung continuum emission [49]. Results of calculations of $\overline{P}_0$, g, and P_0 according to Eqs. (15)–(17) are presented in Figs. 5–7. A comparison reveals that for energies E_1 and temperatures T_1 of the nonthermal electrons close to the excitation energy $E_{\rm ex}$ of the line, both types of energy spectra give the same degree polarization P_0 of about 0.3 for electron temperatures of $T_e<5\times10^6$ K. At higher temperatures the spectrum of Eq. (18) provides larger values of P_0.

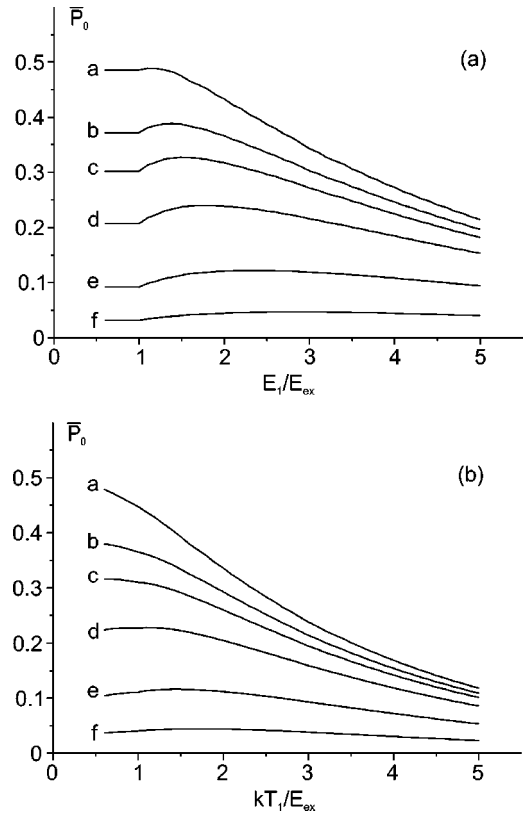

FIG. 5. Calculations of the degree of polarization $\overline{P}_0$ according to Eqs. (14) and (15) of the resonance line of Al XII ions excited by a beam of electrons with $f_{\rm nt}(\varepsilon)$. (a) Case of the exponential spectrum (model A) according to Eq. (18) with the index $\gamma=4.5$ as function of the energy E_1 in units of the excitation energy $E_{\rm ex}$ of the line. (b) Case of model B with a hot Maxwellian with kT_1, also in units of $E_{\rm ex}$. The curves denoted by the labels *a* through *f* correspond to the values of $E_0/E_{\rm ex}=0.1$, 0.3, 0.5, 1, 3, and 10, respectively. The calculations of the factor g from Eq. (17) were made with $X=\langle v\sigma\rangle_{\rm th}$.

B. Polarization calculations

For calculations of the polarization degree of lines excited by a unidirectional electron beam as well as of the parameters β and g, the excitation cross-sections for the M sublevels were obtained in the Coulomb-Born exchange approximation with the help of the ATOM code (see Ref. [14]). For a monoenergetic electron beam the values agree with those of Ref. [30] to within 5%, which were obtained by calculations in the DW approximation. For the calculations of the factor g we used the collisional-radiative model described in Ref. [50]. In addition to direct electron impact excitation, cascades from excited states, radiative, three-body and dielectronic recombination, resonance scattering contributions as well as ionization processes leading to the formation of the *w* and *y* lines were taken into account.

For Al ions with nuclear spin $I=\frac{5}{2}$, the depolarization effect of hyperfine interactions should be accounted for. As was shown in Ref. [30], this effect considerably decreases (by a factor of more than 5) the polarization of the intercombination line (y), but has practically no influence on the *w*-line. In addition, with increasing electron density fast inelastic collisions between the $n=2$ triplet states by the isotropic Maxwellian electrons further reduce the polarization degree of the intercombination line, and it practically vanishes.

C. Interpretation of experimental results

The experimental double intensity ratio K displayed in Fig. 4 as function of the angular dependence ϕ shows $K>1$ for all angles where the planes of incidence of both spectrographs do not coincide. This definitely proves polarization of the *w* line, the *y* line being unpolarized, provided of course that the *w* line is not optically thick. We shall address this problem below. Employing χ^2 minimization, the data points are finally fitted with the theoretical angular dependence according to Eqs. (4) and (5), yielding a value of

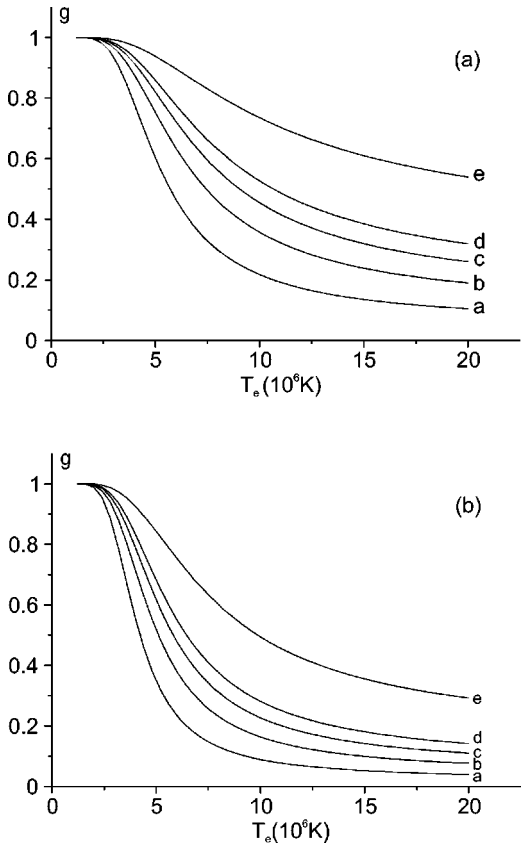

FIG. 6. Dependence of the factor g on the electron temperature T_e (in K) of the bulk plasma. (a) $f_{\mathrm{nt}}(\varepsilon)$ corresponds to the exponential spectrum with $E_1=E_{\mathrm{ex}}$ and (b) $f_{nt}(\varepsilon)$ corresponds to a high-temperature Maxwellian with $kT_1=E_{\mathrm{ex}}$. The labels a through e on both graphs correspond to relative densities of the nonthermal electrons $n_{\mathrm{nt}}=0.5$, 1, 1.5, 2, and 5 (%), respectively.

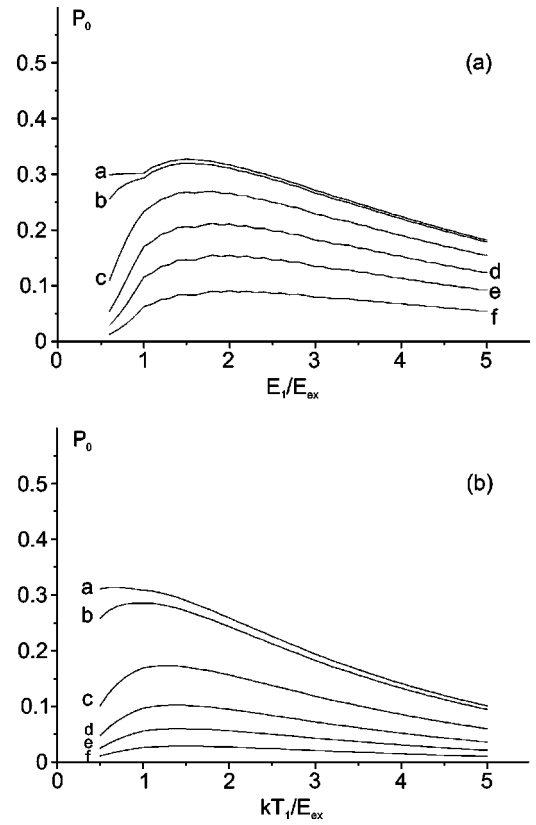

FIG. 7. Calculation of the degree of polarization P_0 according to Eq. (17) for the resonance line (w) of Al XII ions excited by nonthermal electrons in a plasma with a relative density $n_{\mathrm{nt}}=1\%$. (a) Case of an exponential spectrum according to Eq. (18) with the index $\gamma=4.5$ as function of the energy E_1 in units of the excitation energy E_{ex} of the line. (b) Case of a hot Maxwellian with kT_1 also in units of E_{ex}. The curves denoted by the labels a through f correspond to electron temperatures of the bulk plasma of $T_e=2$, 3, 5, 7, 10, and 20 (10^6 K), respectively.

$P_0=0.12\pm0.015$ for the polarization of the y line. In order to derive information on the distribution function of the anisotropic electrons, however, a detailed self-consistent analysis of the spectra has to be made.

For this we consider, in addition to the w and y lines as reference, also the groups of their [Li]-ion satellites identified in the spectra: $j+k,q+r,a+d+c$, and those radiating from $1s2p3l$ states. We simply denote them by j, q, a, and $3l$, respectively. For the analysis we use the spectra recorded with the fixed reference spectrograph, and look for changes of relative intensities of those lines. The intensity ratios $3l/j$, q/j, q/a, j/y, and y/w are formed, the averaged values derived from the spectra being 0.7, 0.73, 1.11, 0.26, and 0.38, respectively. They all show variations, which can be naturally connected with changes of the plasma parameters. The most noticeable change (by a factor of up to 2) is observed for the ratio $3l/j$, while the variations of the other ratios remain within 20% of their average values. Remarkably, these variations are correlated with each other — an increase in one ratio is correlated with an increase of all other ratios. However, neither the averaged values nor their variations can be described by quasi-steady-state or transient (ionizing) thermal models usually used in the analysis of the spectra.

The line intensity ratio $3l/j$, sensitive only to the electron temperature T_e, indicates a value about $1.5-2$ times larger than the temperature from the ratio j/y of about 600 eV, even if accounting for a possible reduction of the y line due to the high density effect. In order to explain the y/w ratio one needs an electron density of about 3×10^{20} cm^{-3}. At such densities it is also impossible to interpret a high value of the intensity ratio j/y in a recombination regime of the plasma, since the intensity ratio q/j of the satellites is high, and for this observation one has to invoke a very low ionization temperature of about 150 eV. The observations thus remain contradictory and inconsistent within thermal models.

On the other hand, a nonthermal model A [Eq. (18)] based on a Maxwellian bulk plasma and a small admixture of about 1% of anisotropic non-Maxwellian electrons allows the interpretation of all features in the spectra mentioned above, as well as of the polarization of the w line. The enhancement and variation in the $3l/j$ ratio can be naturally attributed to such electrons with a low cutoff energy E_1 close to the excitation energy of the $n=3$ satellite group, which is of the order of 1.4 keV. The decrease of the y/w ratio is then connected with preferential excitation of the singlet line relative to the triplet lines due to the difference in the energy dependence of excitation cross sections. The q/j and q/a ratios are now also in quantitative agreement, suggesting an ionization temperature of about 250 eV.

The electron temperature is reduced to about 350 eV, and comes close to the ionization temperature. Such a difference in these temperatures is quite natural, since the electron density should be less than 10^{20} cm^{-3} according to this model, and the ionization equilibrium, therefore, will lag behind the electron temperature. The low electron density of 10^{20} cm^{-3} or even less is consistent with the observations of Ref. [51], when a low-inductance vacuum spark is operated at relatively low currents and low initial line density.

The assumptions of the model described above also allow derivation of the parameters of the nonthermal electrons from the polarization measurements by utilizing Eqs. (15)–(17). Calculations show that a parameter E_0 of about $E_0 = 3E_{ex} \approx 5$ keV is necessary to explain the measured polarization of the *w* line. The average pitch angle near the maximum energy of the nonthermal electrons then is $\alpha_0 = 50°$. We note that the two-temperature model B fails to describe the observed intensities because of the absence of the low-energy cutoff. It may be astonishing, but both the picture of a developing micropinch in the visible [48] as well as numerical modeling of the $m=0$ instability in a pinch column [52] display a density structure corresponding to a double cone with a cone angle of $2\alpha_0 \approx 100^0$.

We finally consider the optical thickness of the *w* line since it may reduce its degree of polarization although it actually does not explain the variation of the ratio *K*. Both spectrographs are carefully aligned opposite each other and view the same plasma: any change due to absorption of the intensity of an unpolarized *w* line would be recorded to the same degree by both instruments and cancel in the ratio. For an electron density of 10^{20} cm^{-3} and a width given by Doppler broadening corresponding to the plasma temperature, we estimate an optical depth of $\tau \approx 1$. In addition, heliumlike lines are emitted during the compression phase where the plasma is highly dynamical: locally varying radial velocities thus introduce additional Doppler shifts of the lines, reducing any absorption further. We therefore safely conclude that optical depth effects do not play a role in our observation and its interpretation.

IV. CONCLUSION

The application of x-ray polarization spectroscopy to the study of micropinches in vacuum spark plasmas revealed the presence of anisotropic high-energy electrons. A polarization degree of $P_0 = 0.12$ was obtained for the resonance line of the Al XII ions. A self-consistent model was developed for the analysis of the spectra, and allowed the derivation of parameters of the energy spectrum and the anisotropy of the electrons.

ACKNOWLEDGMENTS

This work was supported by the Deutsche Forschungsgemeinschaft and at the Lebedev Institute by the INTAS-RFBR under Grant No. 95-0875 and the RFBR under Grant No. 97-02-16919. The authors acknowledge fruitful discussions with O. Herzog and K. N. Koshelev.

[1] D. J. S. Green, J. L. Shohet, and P. I. Raimbault, Phys. Rev. Lett. **27**, 90 (1971).
[2] J. L. Shohet, D. B. van Hulsteyn, S. J. Gitomer, J. F. Kephart, and R. P. Godwin, Phys. Rev. Lett. **38**, 1024 (1977).
[3] S. von Goeler, J. Stevens, W. Stodiek, S. Bernabet, M. Bitter, T. K. Chu, K. W. Hill, D. Hillis, W. Hooke, F. Jobes, G. Lenner, E. Meservey, R. Motley, N. Sauthoff, S. Sesnic, and F. Tenney (unpublished).
[4] M. Lamourex, in *Advances in Atomic, Molecular and Optical Physics*, edited by D. Bates and B. Bederson (Academic, New York, 1993), Vol. 31, p. 223.
[5] I. P. Tindo, V. D. Ivanov, S. L. Mandelshtam, and A. I. Shurigin, Sol. Phys. **24**, 429 (1970).
[6] B. V. Somov and I. P. Tindo, Kosm. Issled. **16**, 686 (1987).
[7] E. Haug, Sol. Phys. **61**, 129 (1979).
[8] E. Haug, Sol. Phys. **71**, 77 (1981).
[9] A. M. Urnov, J. Phys. B **28**, 1 (1994).
[10] V. V. Krutov, V. V. Korneev, S. L. Mandelshtam, A. M. Urnov, and I. A. Zhitnik (unpublished).
[11] A. S. Shlyaptseva, A. M. Urnov, and A. V. Vinogradov, and P. N. Lebedev (unpublished).
[12] V. V. Korneev, S. L. Mandelshtam, S. N. Oparin, A. M. Urnov, and I. A. Zhitnik, Adv. Space Res. **2**, 139 (1983).
[13] I. A. Zhitnik, V. V. Korneev, V. V. Krutov, S. N. Oparin, and A. M. Urnov, Tr. Fiz. Inst. Akad. Nauk SSSR **179**, 39 (1987). English translation in *X-Ray Spectroscopy and Properties of Multiply Charged Ions, Proceedings of the Lebedev Physics Institute*, edited by I. I. Sobelman (Nova, New York, 1988), Vol. 179, p. 51.
[14] A. S. Shlyaptseva, A. M. Urnov, and A. V. Vinogradov, P. N. Lebedev Physical Institute of the USSR Academy of Sciences, Report No. 194, Moscow, 1981 (unpublished).
[15] A. V. Vinogradov, A. M. Urnov, and A. S. Shlyaptseva, Tr. Fiz. Inst. Akad. Nauk SSSR **195**, 89 (1989). English translation in *Atomic and Ionic Spectra and Elementary Processes in Plasma. Proceedings of the Lebedev Physics Institute of Russian Academy of Sciences*, edited by I. I. Sobelman (Nova, New York, 1992), Vol. 192, p. 93.
[16] A. M. Urnov (unpublished).
[17] M. K. Inal and J. Dubau, J. Phys. B **20**, 4221 (1987); **22**, 3329 (1989).
[18] S. Fineschi and E. L. Degl'Innocenti, Astrophys. J. **392**, 337 (1992).
[19] V. L. Jacobs and A. B. Filuk, in *Laser and Particle Beams* (Cambridge University Press, New York, 1995), Vol. 13, p. 303.
[20] T. Fujimoto, H. Sahara, G. Csanak and S. Grabbe (unpublished).
[21] J. Mitroy, Phys. Rev. A **37**, 649 (1988).
[22] J. Mitroy and D. W. Norcross, Phys. Rev. A **37**, 3755 (1988).
[23] H. L. Zhang, D. H. Sampson, and R. E. H. Clark, Phys. Rev. A **41**, 198 (1990).
[24] T. Fujimoto, F. Koike, K. Sakimoto, R. Okasawa, K. Kawasaki, K. Takiyama, T. Oda, and T. Kato (unpublished).

[25] J. R. Henderson, P. Beiersdorfer, C. L. Lennet, S. Chantrenna, D. P. Knapp, R. E. Marrs, G. A. Doschek, J. F. Seely, C. M. Brown, R. LaVilla, J. Dubau, and M. A. Levine, Phys. Rev. Lett. **65**, 705 (1990).

[26] P. Beiersdorfer, D. A. Vogel, K. J. Reed, V. Decaux, J. H. Scofield, K. Widmann, G. Holzer, E. Forster, O. Wehrhan, D. W. Savin, and L. Schweikhard, Phys. Rev. A **53**, 3974 (1996).

[27] J. Dubau, Y. Garbuzov, and A. Urnov, Phys. Scr. **49**, 39 (1994).

[28] K. Akita, K. Tanaka, and T. Watanabe, Sol. Phys. **86**, 101 (1983).

[29] V. A. Veretennikov, A. E. Gurei, A. N. Dolgov, V. V. Korneev, and O. G. Semenov, Pis'ma Zh. Éksp. Teor. Fiz. **47**, 29 (1988) [JETP Lett. **47**, 35 (1988)].

[30] J. C. Kieffer, J. P. Matte, H. Pepin, M. Chaker, Y. Beadoin, T. W. Johnston, C. Y. Chien, S. Coe, G. Mourou, and J. Dubau, Phys. Rev. Lett. **68**, 480 (1992).

[31] J. C. Kieffer, J. P. Matte, M. Chaker, Y. Beaudoin, C. Y. Chien, S. Coe, G. Mourou, J. Dubau, and M. K. Inal, Phys. Rev. E **48**, 4648 (1993).

[32] T. Fujimoto, H. Sahara, T. Kawachi, T. Kallstenius, M. Goto, H. Kawase, T. Furukubo, T. Maekawa, and Y. Terumichi, Phys. Rev. E **54**, R2240 (1996).

[33] O. Herzog, G. Bertschinger, M. Bitter, J. Weinheimer, A. Urnov, F. B. Rosmej, H.-J. Kunze (unpublished).

[34] T. Fujimoto and S. Kazantsev, Plasma Phys. Controlled Fusion **39**, 1267 (1997).

[35] F. B. Rosmej, J. Quant. Spectrosc. Radiat. Transf. **51**, 319 (1994).

[36] A. V. Gurevich and Yu. N. Zhivlyuk, Zh. Éksp. Teor. Fiz. **49**, 214 (1965) [Sov. Phys. JETP **22**, 153 (1966)].

[37] A. V. Gurevich and Ya. N. Istomin, Zh. Éksp. Teor. Fiz. **77**, 923 (1979) [Sov. Phys. JETP **50**, 470 (1979)].

[38] B. V. Somov, *Physical Processes in Solar Flares* (Kluwer, Dordrecht, 1992), p. 258.

[39] V. V. Pustovalov, V. P. Silin, and V. T. Tichonchuk, Pis'ma Zh. Éksp. Teor. Fiz. **17**, 120 (1973) [JETP Lett. **17**, 84 (1973)].

[40] K. N. Koshelev and N R. Pereira, J. Appl. Phys. **69**, R21 (1990).

[41] V. V. Vikhrev, V. V. Ivanov, and K. N. Koshelev, Sov. J. Plasma Phys. **8**, 688 (1982).

[42] A. Schulz, M. Hebach, H.-J. Kunze, F. B. Rosmej, and F. Walden, J. Quant. Spectrosc. Radiat. Transf. **51**, 341 (1994).

[43] T. J. Welch and E. J. Clothiaux, J. Appl. Phys. **45**, 3825 (1974).

[44] R. Beier, C. Bachmann, and R. Burhenn, J. Phys. D **14**, 643 (1983).

[45] K. Blum, *Density Matrix Theory and Applications* (Plenum, New York, 1981).

[46] V. B. Berestetskii, E. M. Lifshitz, and L. P. Pitaevskii, *Quantum Electrodynamics* (Pergamon, Oxford, 1982).

[47] R. Novick, Space Sci. Rev. **18**, 389 (1975).

[48] Ch. K. Erber, O. H. Herzog, A. Schulz, E. J. Clothiaux, F. Walden, and H.-J. Kunze, Plasma Sources Sci. Technol. **5**, 436 (1996).

[49] R. Beier and H.-J. Kunze, Z. Phys. A **285**, 347 (1978).

[50] I. L. Beigman, S. N. Oparin, A. M. Urnov, Tr. Fiz. Inst. Akad. Nauk SSSR **195**, 47 (1989). English translation in *Atomic and Ionic Spectra and Elementary Processes in Plasma. Proceedings of the Lebedev Physics Institute of Russian Academy of Sciences*, edited by I. I. Sobelman (Nova, New York, 1992), Vol. 192, p. 51.

[51] F. S. Antsiferov, K. N. Koshelev, E. A. Kramida, and A. M. Panin, J. Phys. D **22**, 1073 (1989).

[52] V. V. Vikhrev, V. V. Ivanov, and G. A. Rozanova, Nucl. Fusion **33**, 311 (1993).